# Chapter – 2

# *Nuclear Properties and Theoretical Models*

## 2.1. Properties of Electromagnetic Radiation and Nucleus

### 2.1.1. Multipolarity of Electromagnetic Radiation

Static (i.e., constant in time) distributions of charges and currents give static electric and magnetic fields. If the charge and current distributions vary with time, a radiation field is produced and electromagnetic radiation is emitted. A classical description of the electromagnetic radiation can give a simple understanding of its basic properties. Any distribution of electric charge and currents produces electric and magnetic fields vary with distance in a characteristic fashion. It is customary to assign to the charge and current distribution a *multipole* moment associated with each characteristic spatial dependence - the $1/r^2$ electric field arises from the net charge (*monopole* moment), the $1/r^3$ electric filed arises from the electric dipole (*dipole* moment, d=q*l*), the $1/r^4$ electric field arises from an ellipsoid charge distribution (*quadrupole* moment), and so on. The change of the value of a particular moment creates radiation of the same type as this moment. For instance oscillation in the value of the electric dipole moment (for instance by changing the distance between the positive and negative charges, *l*) creates electric dipole radiation, while changing the magnetic dipole moment ($\mu$ = iA, for instance by changing the current, i, in the circular loop area A) creates magnetic dipole radiation.

#### 2.1.1.1. Electric Quadrupole Moment

The electric quadrupole operator is defined in terms of the nuclear charge density distribution $\rho(r)$:

$$eQ(r) = \int \rho(r) r (3Cos^2\theta - 1) dr, \qquad (2.1)$$

where, r is the radius vector and $\theta$ if the angle it subtends. The integral vanishes for spherically symmetric charge distributions and thus only a deformed nucleus will have a static quadrupole moment. The intrinsic quadrupole moment is defined [1] in terms of the deformation parameter $\beta_2$:

$$Q_0 = \frac{3}{\sqrt{5\pi}} ZR^2\beta_2, \qquad (2.2)$$

where, R is approximated by $R \cong 1.23A^{1/3}$fm. For a nucleus with prolate (oblate) deformation, $Q_0$ is positive (negative). The reduced transition strength B(E2) for a quadrupole transition linking states of spins *I* and *I-2* is given by the expression

$$B(E2) = \frac{5}{16\pi} Q_0^2 \langle IK20|I-2K\rangle^2 (eb)^2, \qquad (2.3)$$

this in turn is related to the transition probability by

$$T_{fi} = \frac{12\pi}{225\hbar}\left(\frac{E_\gamma}{\hbar c}\right)^2 B(E2), \qquad (2.4)$$

The measurement of reduced E2 transition strengths thus lead to information about the overall deformation of the nucleus.

### 2.1.1.2. Magnetic Dipole Moment

Classically, the nuclear magnetic field is the product of two phenomena: the orbital motion of the protons which constitutes a current, and the intrinsic spin of the nucleons. Even for the neutron, there is an intrinsic magnetic dipole moment associated with its internal quark structure. Measured M1 strengths thus provide a probe into nuclear currents and hence the single-particle structure.

The reduced transition strength B(*MI*) for stretched magnetic dipole (*MI*) transitions linking states with spins *I* and *I* - *1* is defined in terms of the nuclear g-factors:

$$B(M1) = \frac{3}{4\pi}(g_K - g_R)^2 K^2 \langle IK10|I-1K\rangle^2 \mu_N^2, \qquad (2.5)$$

where, $\mu_N = \frac{e\hbar}{2mc}$ is the nuclear magneton. The rotational g-factor $g_R$ describes the current arising from the collective rotation of the core:

$$\mu = g_R R \mu_N, \qquad (2.6)$$

and can be approximated by $g_R \cong Z/A$ although in practice this represents an upper limit for $g_R$. On the other hand the intrinsic g-factor $g_k$ describes the currents which arise from the orbital motion of the valance nucleons:

$$g_K = g_l + \frac{1}{\Omega}(g_s - g_l)\langle\Omega|s_z|\Omega\rangle, \qquad (2.7)$$

The total magnetic dipole moment μ for total angular momentum I = R + j is given by

$$\mu = \left(g_R I + (g_K - g_R)\frac{K^2}{K+1}\right)\mu_N, \qquad (2.8)$$

The reduced transition strength B(*MI*) is related to the transition probability $T_{fi}$ as follows:

$$T_{fi} = \frac{16\pi}{9\hbar}\left(\frac{E_\gamma}{\hbar c}\right)^3 B(M1), \qquad (2.9)$$

### 2.1.2. Nuclear shape parameterization

Nuclear shape determines to a large extent the possible nuclear motion modes. Therefore, a convenient shape parameterization for the nucleus is necessary and can be based on the surface, expressed by the radius vector, R;

$$R = R(\theta, \phi), \tag{2.10}$$

$$= R_0\left(1 + \sum_{\lambda=0}^{\infty} \sum_{\mu=-\lambda}^{\lambda} \alpha_{\lambda\mu}\, Y_{\mu\lambda}(\theta, \phi)\right), \tag{2.11}$$

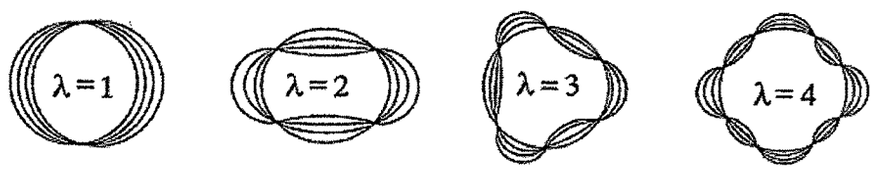


Figure 2.1: Diagrammatic illustration of the multipole deformation for λ = 1, 2, 3, and 4.

R is defines in spherical coordinates to point from the centre of a nucleus to its surface and $Y_{\mu\lambda}(\theta, \phi)$ are the spherical harmonics. The coefficients, $\alpha_{\lambda\mu}$ describe the changes of the nuclear volume with λ defining the deformation type. Examples illustrating the: (λ = 1) dipole, (λ = 2) quadrupole, (λ = 3) octupole and (λ = 4) hexadecapole deformation are shown in Fig. 2.1. μ is an integer varying from -λ to +λ. For the axially symmetric nucleus with quadrupole deformation the five coefficients namely,

$$\alpha_{2m} : \alpha_{21}, \alpha_{22}, \alpha_{20}, \alpha_{2\text{-}1}, \alpha_{2\text{-}2},$$

reduce to only two ($\alpha_{20}$ and $\alpha_{22} = \alpha_{2\text{-}2}$). The other ($\alpha_{21} = \alpha_{2\text{-}1}$) terms vanish. The coefficients, $\alpha_{20 \text{ and } 22}$ are related to the $\beta_2$ and γ parameters according to:

$$\alpha_{20} = \beta_2 cos\gamma, \tag{2.12}$$

and

$$\alpha_{22} = \frac{1}{\sqrt{2}}\beta_2 sin\gamma, \tag{2.13}$$

The parameters, $\beta_2$ and γ define the extent of quadrupole deformation and deviation from an axially symmetric shape respectively.

The equation for the nuclear surface which involves the $\beta_2$ and γ parameters is given by:

$$R(\theta,\phi,\gamma) = R_0\left(1+\beta_2\sqrt{\frac{5}{16\pi}}\left(cos\gamma(3cos^2\theta-1)+\sqrt{3}sin\gamma sin^2\theta cos2\theta\right)\right) \quad (2.14)$$

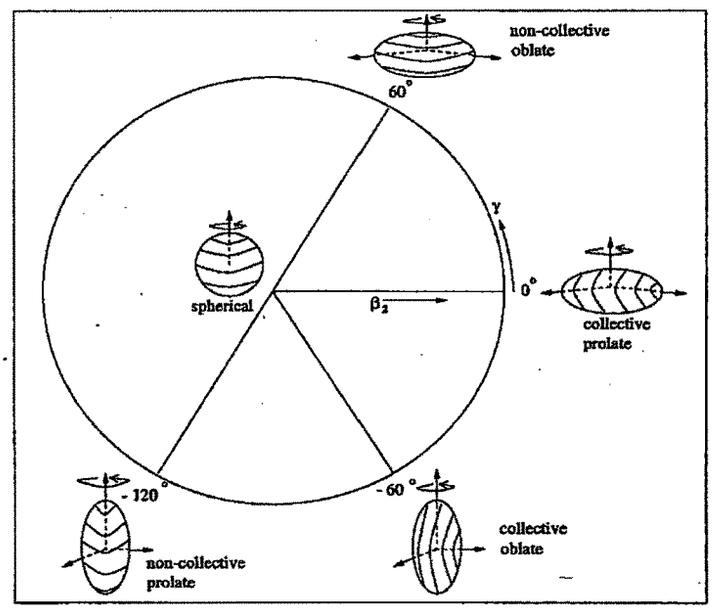


Figure 2.2: Diagrammatic illustration of the Lund convention [2] for various shapes ($\lambda$ = 2) of the rotating nucleus in the ($\beta_2$,$\gamma$) plane.

The nuclear shapes which correspond to various ($\beta_2$,$\gamma$) co-ordinates for $\lambda$=2 are diagrammatically illustrated in Fig. 2.2. The prolate shape corresponds to $\gamma$ = 0° and -120°, while am oblate shape correspond to $\gamma$ = 60° and -60°. The maximum collectivity is observed for -60° ≤ $\gamma$ ≤ 0° while non-collectivity occurs for shapes with $\gamma$ = -120° and $\gamma$ = 60°. In accordance with the Lund convention [2] rotation occurs around the smallest, the intermediate and the largest axis which correspond to the three 0° ≤ $\gamma$ ≤ 60°, -60° ≤ $\gamma$ ≤0° and -120° ≤ $\gamma$ ≤ -60° sectors respectively.

### 2.1.3. Rotational Behaviour of a Nucleus – Rotational Band

The most collective behaviour known in nuclei is the collective rotation, that occur when the nuclear shape becomes appreciably non spherical. Non spherical shapes are due to shell effects in nuclei. For nuclei with proton and/or neutron numbers equal or close to the magic numbers (closed shell) the spherical shape is the most stable. For nucleon numbers

between the magic numbers, the nucleus deforms in order to find a more favourable (i.e., lower) energy. Such deformed shapes allow collective rotations of the nuclei.

A rotational band reflects a collective motion of the nucleus, which changes the orientation of the system, without essentially affecting its shape or intrinsic structure. The energy associated with the motion is kinetic and as follows:

$$E_{exc}(I) = \frac{\hbar^2}{2J_0} I(I+1), \tag{2.15}$$

where, $E_{exc}(I)$ is the excitation energy of the level with angular momentum $I$ from the rotational band. $J_0$ is the moment of inertia and depends on the shape and internal structure of the nucleus. The energy relationship expresses one of the most characteristic features of a rotational motion and applies for a rotation of any rigid body (Fig. 2.3). Rigid body – when all particles of the body take part in the rotation and have the same angular velocity ω, The angular momentum is then $I = \omega J_0$.

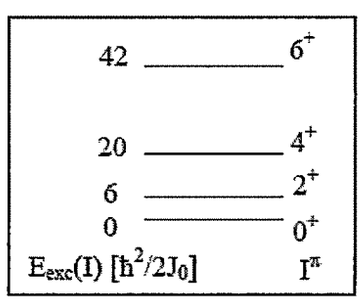


Figure 2.3: Rotation of a rigid body

### 2.1.3.1. Types of Rotational Bands

Depending on the intrinsic configuration, different types of rotational bands are known:

#### a. Ground State Bands of Even-Even Nuclei

They consist of stretched E2 transitions, and are built above the $0^+$ ground state. All the nucleons are paired and the nucleus rotates as a whole around the rotational axis – the axis perpendicular to the symmetry axis of the nucleus (Fig. 2.4).

The spins of the levels of the band are:

$$I^+ = 0^+, 2^+, 4^+, 6^+, \text{etc}$$

The energies of the levels of the band are:

$$E_{exc}(I) = \frac{\hbar^2}{2J_0} I(I+1), \tag{2.16}$$

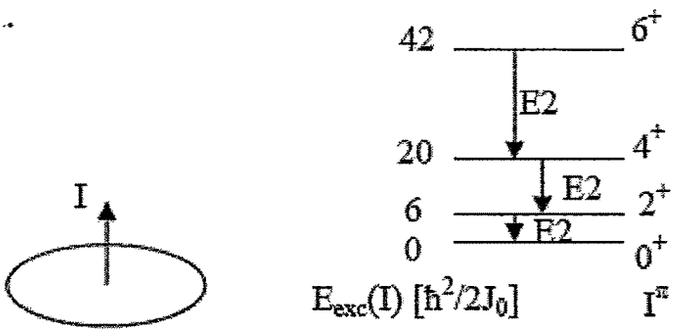


Figure 2.4: Diagrammatic representation of the ground state rotational band in even-even nuclei.

**b. Strongly Coupled bands**

They reflect the rotation of a nucleus with one or more odd nucleons, when the single particle angular momentum $\vec{j}$ is coupled to the collective rotation of the nucleus $\vec{R}$, i.e., the odd particle(s) rotate together (with the same phase) with the nucleus, as shown in Fig. 2.5. Then the projection $\vec{j}$ on the symmetry axis of the nucleus, K, is a good quantum number. These bands are observable for relatively large nuclear deformation with not very high rotational frequencies. The bands contain stretched M1 and E2 transitions. The angular momenta of the levels are: I = K, K+1, K+2, K+3, etc

And the excitation energies are:

$$E_{exc}(I) = \frac{\hbar^2}{2J_0}[I(I+1) - K^2], \text{ if } K \neq ½, \tag{2.17}$$

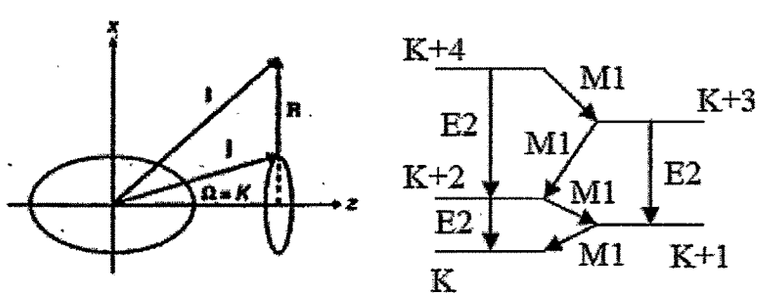


Figure 2.5: Strongly coupled bands

**c. Decoupled Bands**

They reflect the rotation of a nucleus with one or more odd nucleons, for which the odd particles are decoupled from the nuclear rotation, i.e. their angular momentum $\vec{j}$ is aligned along the rotation axis, and their motion is independent from the rotation of the nucleus (Fig. 2.6). The band consists of $\vec{j}$ along the rotation axis, $I$, is a good quantum number and is called alignment. The projection of $\vec{j}$ along the rotation axis $I_x$ is called aligned angular momentum. The spins of the levels of the band are:

$$I = i, i+2, i+4, \text{etc}$$

The energies of the states (relative to the energy of the bandhead level with spin I = i) are:

$$E_{exc}(I) = \frac{\hbar^2}{2J_0}[(I-i)(I-i+1)], \qquad (2.18)$$

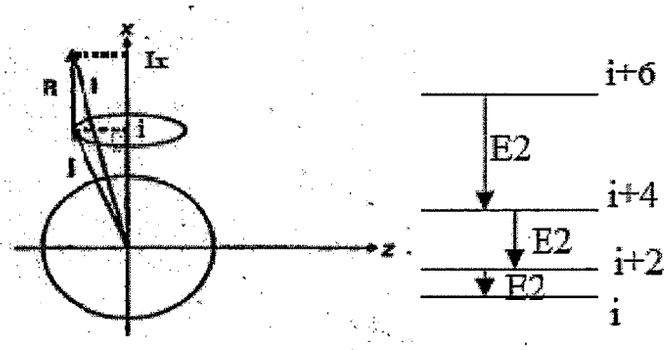


Figure 2.6: Decoupled band

**d. Backbending**

At high rotational frequencies the Coriolis force become strong enough to break nucleon pair. Let us consider for example the rotation in even-even nucleus.

The excitation energy and spin in the ground state band (g), (see Fig.2.7) are gained from faster rotation. At spins 8 – 12$\hbar$ the ground band is crossed by an excited band (e). The Corriolis force at spins 8 – 12$\hbar$ is able to break a pair of nucleons, thus the excited band is associated with different intrinsic configuration. One can see on the plot of the excitation energy as a function of spin (Fig. 2.8) that for low spins the g band is yrast (yrast means that the excitation energy is lowest for that particular spin). At high spins (I > 12$\hbar$ in this case) the band is yrast. At I ~ 10$\hbar$ the two bands cross each other.

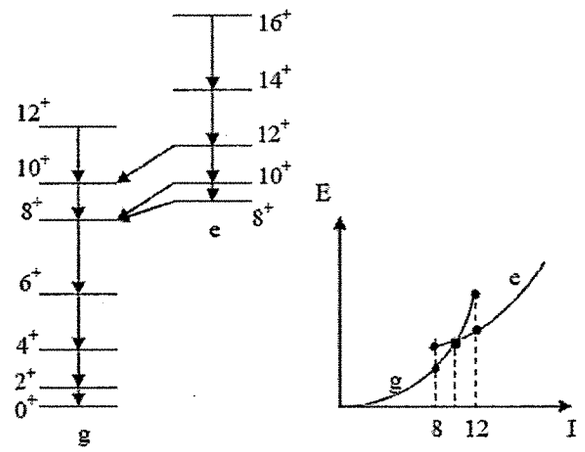


Figure 2.7, 2.8: Figure illustrating backbending phenomenon

The aligned angular momentum $I_x$ for these bands is shown in Fig. 2.19. One can see that $I_x$ for the $g$ band increases with rotational frequency. At the region of the bandcrossing (for $\hbar\omega \sim \hbar\omega_{bc}$) a pair of nucleons breaks, the nucleons' spins align along the rotation axis contributing aligned angular momentum of $i_0$ to the $I_x$ of the excited band. $i_0$ is called alignment. It is the aligned angular momentum $I_x$ of the excited pair at $\hbar\omega = 0$. Thus, in the region of the bandcrossing (bc) the nuclear rotation slows down from $\hbar\omega_2$ to $\hbar\omega_1$. Then, angular momentum is gained again by increasing the rotational frequency (along the excited band). The alignment $i_0$ and the bandcrossing frequency $\hbar\omega_{bc}$ (approximate value for it can be obtained by $\hbar\omega_{bc}=1/2(\hbar\omega_2+\hbar\omega_1)$ are very important quantities, because they can indicate the configuration of the excited band. If for instance two $i_{13/2}$ nucleons get aligned, they will have maximum projections of $\vec{j}$ along the rotation axis of $13/2\hbar$ and $11/2\hbar$ (because they cannot have all quantum numbers the same, thus one will have smaller alignment than the other), thus the alignment will be $i_0 = 13/2 + 11/2 = 12\hbar$.

The bandcrossing frequency has also characteristic values depending on the configuration of the excited nucleons, and also on other parameters, such as nuclear deformation, pairing gap, etc. Since the plot of $I_x$ against the rotational frequency (Fig. 2.9) shows a turn backwards (corresponding to the slowing down of the nuclear rotation) the phenomenon is called a backbending. The moments of inertia and in particular $J^{(2)}$ are very sensitive even to small changes in the intrinsic structure and show sharp changes in the bandcrossing region. Thus, successful nuclear model describing nuclear rotation

should be able to predict such quantities as nuclear configurations, alignments, bandcrossing frequencies, moments of inertia, etc.

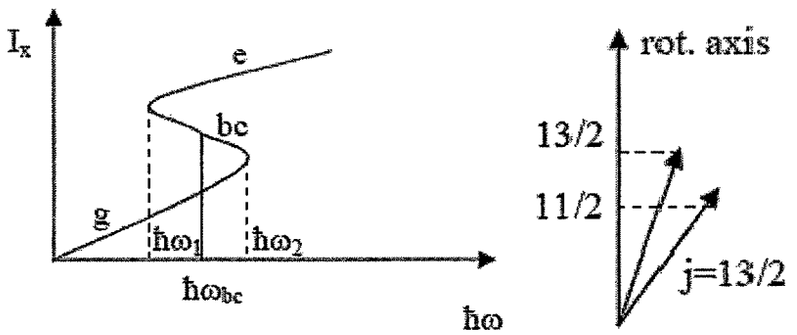


Figure 2.9: Schematic description of Backbending phenomenon

## 2.2. Theoretical Nuclear Models

Many models have been proposed to describe the structure of the nucleus. The nucleus itself is a system of particles where the number of particles is too large to derive a direct solution analytically and too small to use statistical methods to any degree of accuracy [3]. The modern era of nuclear physics began with the surprising revelation that, despite the violent forces that are present in the nucleus, the nucleons can for the most part be considered to be moving independently in a single, smoothly varying force field. This is the conceptual basis of the many nuclear models, which is the foundation for much of our quantitative understanding of nuclear energy levels and their properties. In the models such as shell model and liquid drop model, individual nucleons are considered to fill energy states successively, forming a series of nuclear shells that are analogous to the shells formed by electrons in the atom. At the simplest level, the shell model predicts that the nuclei have closed (completely occupied) shells of protons or neutrons should be unusually stable. If a nucleus has one nucleon beyond the closed shell, many of the properties of the nucleus can be attributed to that one nucleon. The models have been developed to incorporate the residual forces among the nucleons that are not included in the smooth field. This has evolved to a valuable tool for understanding and predicting many of the energy levels and their properties such as electromagnetic interactions and decay rates. In this section, a brief outline of the key models used in the interpretation of this work is given.

### 2.2.1. The Spherical Shell Model

The atomic shell model for electrons has been very successful in explaining the patterns observed in the periodic table. Evidence for a similar type of shell structure has also been observed in nuclei. Large discontinuities occur in the neutron binding energies as a function of the nuclear mass, A, and also in the 2p separation energy; that is the energy required to separate two protons from the nucleus. Anomalies are also seen in the abundance of elements as a function of either proton or neutron number [4, 5]. These discontinuities occur at the so-called 'magic numbers' of 2, 8, 20, 28, 50, 82 and 126. The first excited states of nuclei with a magic number of either protons or neutrons are also anomalously high (> 1.5 MeV). All of this suggests that a shell model approach similar to that used in atomic physics can be taken to model the nucleus.

It is assumed that no detailed interactions occur between the nucleons and that each particle moves independently of the other nucleons. Each nucleon experiences the mean field force, which is the average of the interactions of the nucleon with all the other particles. For two nucleons, $i$ and $j$, the potential $V_i$ as a function of radii $r_i$ is described by,

$$V_i(r_i) = \langle \sum_j V(r_{ij}) \rangle, \tag{2.19}$$

where, $r_{ij}$ is the distance between the two interacting nucleons and V is the potential of the interaction. This gives a Hamiltonian of the form,

$$H = \sum_i T_i + \sum_{ij} V(r_{ij}), \tag{2.20}$$

where, $T_i$ is the kinetic energy associated with each of the nucleons.

It can be assumed that the central interaction is much greater than the residual interactions. The most important part of this model is the choice of the central potential, $V(r_{ij})$. The central potential depends only on the distance between interacting nucleons and is a superposition of all the short-range inter-nucleon potentials. Several potentials have been tried, such as the simple square and the harmonic oscillator. However, without a non-central component being included, the correct magic numbers cannot be reproduced. The harmonic oscillator potential gives a good approximation and is useful to consider, as it can be solved analytically. It takes the form of,

$$V(r) = -V + \frac{1}{2} M\omega^2 r^2, \tag{2.21}$$

where, V is the well depth, which can be varied, and ω is the frequency of the simple harmonic motion. $M$ and $r$ are the mass and radii of the oscillator, respectively.

Solving the Schrödinger equation for the harmonic oscillator gives the energy of the $N^{th}$ shell to be,

$$E_N = \left(N + \frac{3}{2}\right)\hbar\omega, \tag{2.22}$$

where, $N$ is the principal quantum number. States of the harmonic oscillator are labelled by $N$, the total angular momentum, $j$ and the intrinsic orbital angular momentum of the nucleons, momentum of the nucleons, $l$. It should be noted that $l$ is normally written in spectroscopic notation where letters replace numbers such that s, p, d, f, g, h, i refer to $|l|$-values of 0, 1, 2, 3, 4, 5, 6, respectively.

The first magic numbers, 2, 8 and 20, are successfully reproduced by this method, but the higher magic numbers are not. Each energy level has a degeneracy of (2j+1). In atomic physics, this degeneracy is lifted by the spin-orbit interaction caused by the interaction of the atomic electron's magnetic moment with the magnetic field generated by the electron's movement about the nucleus. In nuclei, the intrinsic angular momentum of the nucleon, $s$, couples with the orbital angular momentum, $l$, to give the total angular momentum, $j$. Such a coupling introduces a spin-orbit effect for the nucleus, modifying the Hamiltonian such that,

$$V(r) \Rightarrow V(r) + k1.s., \tag{2.23}$$

This means that the force felt by the nucleons is dependent on the direction of their spin. Nucleons with aligned spin and orbital angular momenta will contribute an energy of $+k$, whereas a nucleon with anti-aligned angular momenta will contribute energy of $-k$. The existence of a strong nucleon-nucleon spin-orbit interaction has been established experimentally in proton-proton scattering experiments. The spin-orbit interaction does not violate the spherical symmetry and therefore leaves $l$, $j$ and $j_z$ as good quantum numbers, where $j_z$ is the projection of $j$ onto the z-axis. The addition of such a spin-orbit effect splits the otherwise degenerate levels with $j = l \pm 1/2$. By making the spin-orbit interaction attractive, it explains why $j = l + 1/2$ states lie lower in energy than $j = l - 1/2$ states. The inclusion of the spin-orbit interaction changes the levels of the harmonic oscillator, known as the Modified Harmonic Oscillator (MHO), and the shell gaps reproduce the magic numbers 2, 8, 20, 28, 50, 82 and 126. The splitting of the harmonic oscillator levels is proportional to $l$, which can create states with an "unnatural" parity, and alter the order of the levels. This gives rise to "intruder" states, where states with a higher value of $l$ lie lower in energy than the lower-$l$ states. The differences

between the energy levels reproduced by different oscillator potentials are shown in Fig. 2.10. where, an example of an intruder is at the $h_{11/2}$ orbital.

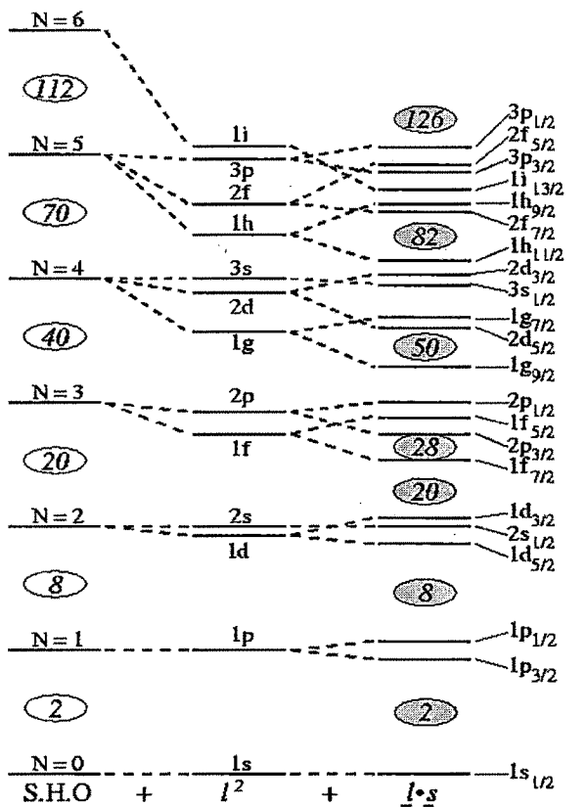


Figure 2.10: The evolution of the states from a simple harmonic oscillator model into a more realistic representation of the nucleus [6]. The 'magic numbers' are marked in the cicles.

The Modified Harmonic Oscillator (MHO) potential has some problems: as r tends to infinity, the potential becomes unphysical, and although the magic numbers are reproduced correctly, the ordering of the levels is not. A more realistic potential is the Woods-Saxon potential, which takes the form of,

$$V(r) = \frac{-V_0}{1+\exp\left[\frac{r-R_0}{a}\right]}, \tag{2.24}$$

where, $R_0$ is the average nuclear radius and a is the skin thickness of the diffuse nuclear surface. This potential closely matches the form of the nuclear charge

distribution, which has been measured experimentally. A comparison of the shapes of the two potentials is shown in Fig. 2.11.

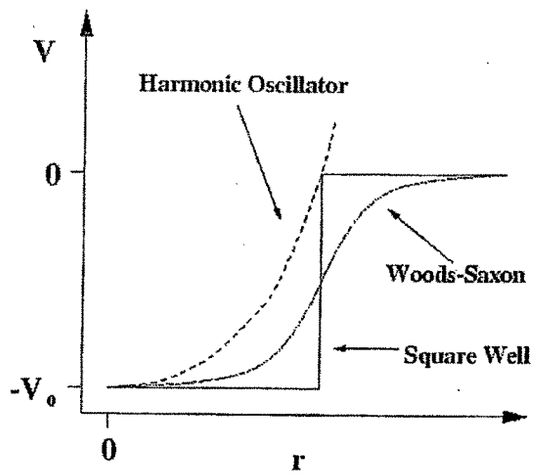


Figure 2.11: A comparison of the different potentials showing a simple square well, the harmonic-oscillator and the Woods-Saxon potentials.

The energy levels produced from solving the Schrödinger equation for the Woods-Saxon potential are very similar to those from the MHO potential, but the ordering of the energy levels is altered, giving a more realistic picture of the nucleus. A comparison between the harmonic oscillator energy levels and the Woods-Saxon energy levels is shown in Fig. 2.12. The spherical shell model describes the properties of closed-shell and light-mass nuclei very well. However, if there are several nucleons outside the closed shell, the shell model predictions cease to match the experimental data and a new description must be sought.

### 2.2.2. The Deformed Shell Model or Nilsson Model

Experimental evidence such as the existence of rotational bands and high values of electric quadrupole moments for certain nuclei suggests that away from closed shell; nuclei must adopt a stable ground state deformation. To construct a model of the nucleus which includes the possibility of deformation, a non-spherical potential must be used. The simplest potential is the Anisotropic Harmonic Oscillator (AHO) potential which forms the basis of the widely used deformed shell model, the Nilsson Model.

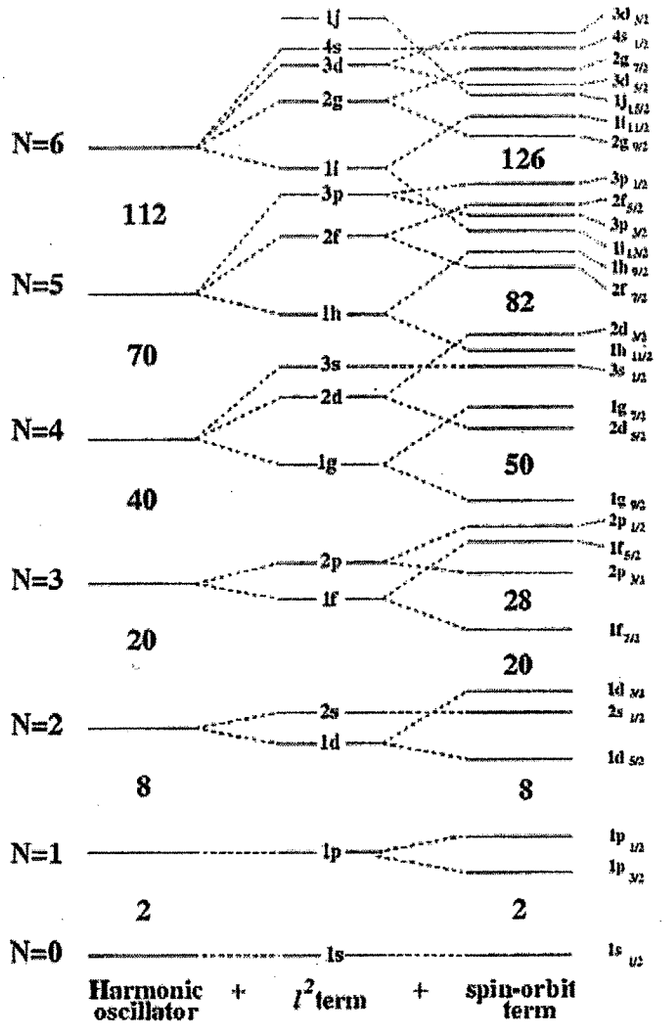


Figure 2.12: A comparison between the energy levels of the harmonic oscillator and Woods-Saxon potentials.

Nuclei away from the closed shells have been found to have large quadrupole moments [7], which suggest a deviation away from the spherical shape [8]. The observation of numerous rotational bands also indicates the existence of non-spherical nuclear shapes as spheres cannot be observed to rotate quantum mechanically.

The projection of the single-particle angular momentum onto the symmetry axis is denoted by $\Omega$ and the projection of the total angular momentum is denoted by $K$. For a nucleus with only one valence particle, the rotational angular momentum of axially symmetric nuclei is perpendicular to the symmetry axis, therefore, it does not contribute

to $K$ and hence, for this system, $K = \Omega$. For a prolate-deformed nucleus, orbits with a low $\Omega$ will have lower energies and high- orbits will have higher energies; the converse is true for oblate nuclei. The angle of the orbital plane, $\theta$, for such a nucleon can be approximated, as shown in Fig. 2.25, by

$$\theta = \sin^{-1}(\frac{K}{j}), \tag{2.25}$$

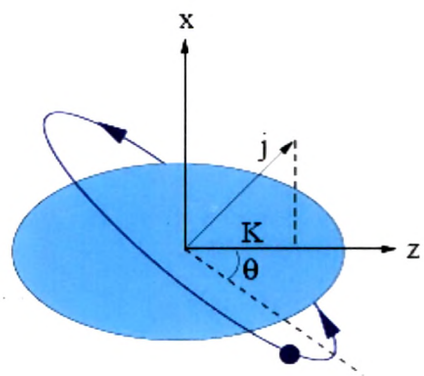


Figure 2.13: Diagram showing the definitions of K and θ for a valance nucleon orbiting in a deformed potential.

For high values of $K$, $\theta$ changes rapidly, but it changes quite slowly for low values of $K$. This, in turn, means that for deformations where $\beta > 0$, the energy falls rapidly as $\beta$ increases for low values of and rises for high values of $\Omega$. The separation of neighbouring $\Omega$ values increases rapidly as $K$ increases. Combining this $\Omega$ splitting with the mixing of states with different $l$ values creates a complex arrangement of the energy levels. Energy levels calculated are called Nilsson orbitals and are represented in a Nilsson diagram as shown in Fig. 2.14. One of the fundamental rules of quantum mechanics is that no two energy levels with the same quantum numbers can cross, so when a line approaches another line with the same $K^{\pi}$, where $\pi$ is the parity, they repel each other. Each line on the diagram represents a different Nilsson state and starts off straight, with either a downwards or upwards slope. When it approaches another level with the same $K^{\pi}$, it starts to curve as seen in the Fig. 2.14. The Nilsson orbitals are normally labelled by,

$$\Omega^{\pi}[Nn_z\Lambda], \tag{2.26}$$

$\Omega^{\pi}$ are the $\Omega$ value and parity, as previously described. N is the principal qauantum number; in an oscillator mode it denotes the number of oscillator quanta, and it gives the number of the major shell. The projection of N onto the symmetry axis (the *z*-axis) is $n_z$, which corresponds to the number of nodes in the wave function in the *z* direction and $\Lambda$ is the projection of *l* on the symmetry axis The deformation of $\Omega$ means that

$$\Omega = \Lambda + \Sigma$$
$$= \Lambda \pm \tfrac{1}{2}, \tag{2.27}$$

as $\Sigma$ is the projection of the intrinsic spin of the nucleon, *s,* onto the symmetry axis. The Nilsson orbits are shown in Fig. 2.14. as a function of deformation and energy.

The deformation parameter $\varepsilon$ is defined as,

$$a = R(1 + \varepsilon),$$
$$b = R/(1 + \varepsilon)^{1/2}, \tag{2.28}$$

Where, *a* and *b* are the major and minor axes of an ellipsoid, respectively, and $\varepsilon$ is closely related to $\beta$ as,

$$\beta = \left(\frac{4\pi}{5}\right)^{1/2} \varepsilon, \tag{2.29}$$

### 2.2.3. Triaxial Nuclear Shapes

The Nilsson deformed shell model provides an excellent single-particle description for well-deformed nuclei, around the mass 130-140 region of the nuclear chart. A variety of prolate and oblate nuclear shapes can be found, but the transitional nuclei between these two shapes need further consideration.

For triaxial nuclei, an anisotropic harmonic oscillator model can be employed to provide a single-particle description, as with axially symmetric nuclei [11]. The harmonic oscillator potential, V, takes the form,

$$V_{HO} = \frac{1}{2} M(\omega_x^2 x^2 + \omega_y^2 y^2 + \omega_z^2 z^2), \tag{2.30}$$

where $\omega_x \neq \omega_y \neq \omega_z$. The relation between the oscillator frequencies can be described in terms of $\varepsilon$ and $\gamma$, the deformation parameters introduced in section 2.2.3,

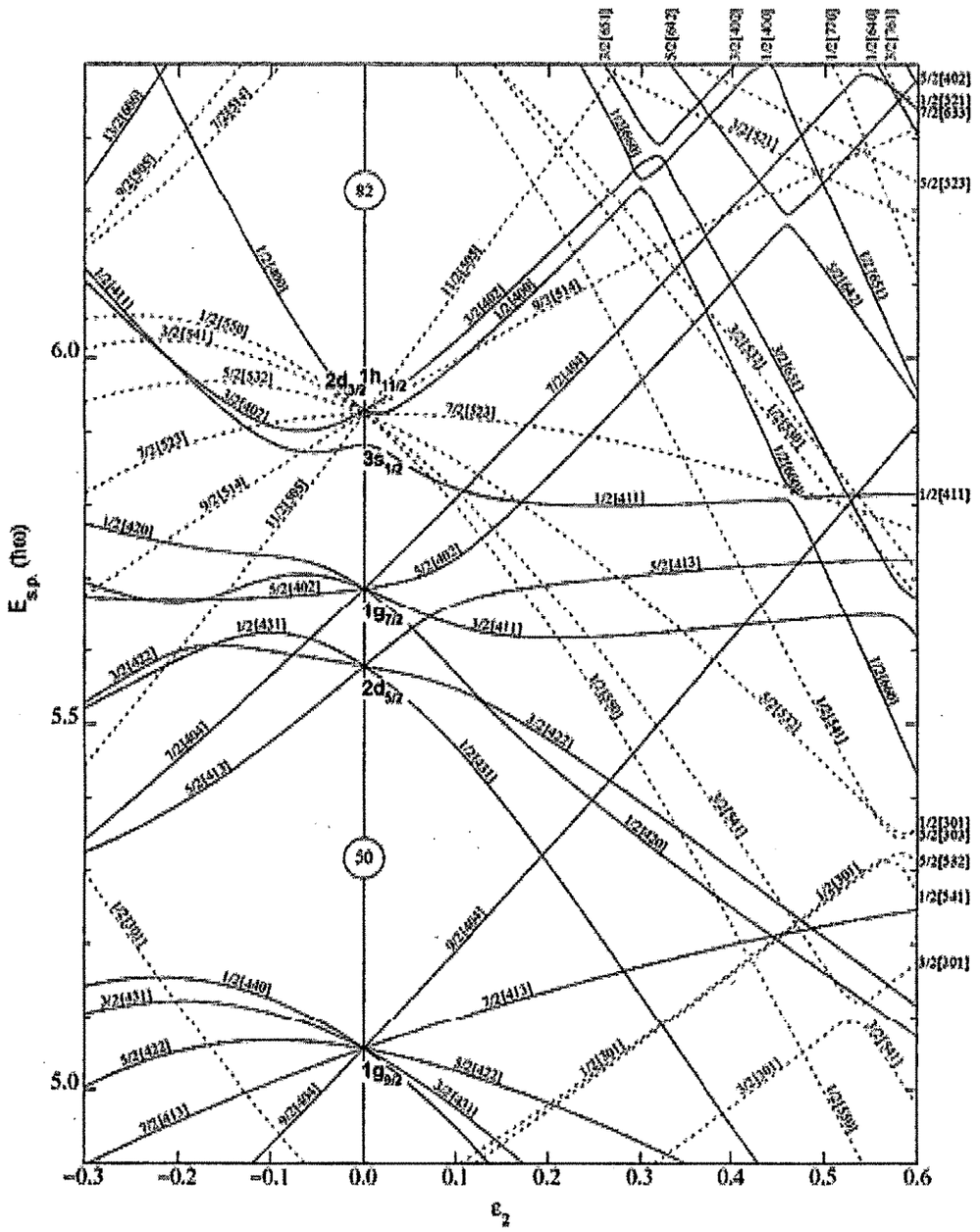


Figure 2.14: Nilsson diagram for neutron orbitals for N=50-82 [9, 10].

$$\omega_x = \omega_0(\varepsilon,\gamma)\left[1-\frac{2}{3}\varepsilon\cos\left(\gamma+\frac{2\pi}{3}\right)\right],$$
$$\omega_x = \omega_0(\varepsilon,\gamma)\left[1-\frac{2}{3}\varepsilon\cos\left(\gamma+\frac{2\pi}{3}\right)\right], \qquad (2.31)$$
$$\omega_x = \omega_0(\varepsilon,\gamma)\left[1-\frac{2}{3}\varepsilon\cos\left(\gamma+\frac{2\pi}{3}\right)\right],$$

where, $\omega_0$ is the harmonic oscillator quantum and for volume conservation, $\omega_0^3 = \omega_x\omega_y\omega_z$. Nilsson [9] employed a set of stretched co-ordinates to describe the nuclear shape, where each coordinate is a stretched transform of the Cartesian equivalent,

$$\xi = x\left(\frac{M\omega_x}{\hbar}\right)^{1/2},$$
$$\eta = y\left(\frac{M\omega_y}{\hbar}\right)^{1/2}, \qquad (2.32)$$
$$\zeta = z\left(\frac{M\omega_z}{\hbar}\right)^{1/2},$$

As with the previous description of a deformed potential, spherical harmonics $Y_{\lambda,\mu}(\theta_t, \phi_t)$, can be used to describe the potential for triaxial shapes, where $\theta_t$ and $\phi_t$are the polar and azimuthal angles, respectively. In the stretched coordinates described in Eq$^{n}$'s 2.31 and 2.32, the potential can be rewritten as

$$V_{HO} = \frac{1}{2}\hbar\omega_0\rho^2\left[1 - \frac{2}{3}\varepsilon\left(\frac{4\pi}{5}\right)^{1/2}\left(\cos(\gamma Y_{20} - \frac{sin\gamma}{\sqrt{2}}(Y_{22} - Y_{2-2})\right)\right], \qquad (2.33)$$

where $\rho^2$, is the nuclear radii in terms of the stretched coordinates,

$$\rho^2 = \xi^2 + \eta^2 + \zeta^2, \qquad (2.34)$$

To give higher order deformations and a more realistic nuclear potential, $l \,.\, s$ and $l^2$ terms can be added to the above potential. The γ-deformation still leaves each orbital filled by two particles moving in different directions in time-reversed orbits. This means that parity is conserved (as long as no λ = 3 terms are included), leaving parity as a good quantum number. Consequently, odd-N and even-N shells remain uncoupled. However, for a triaxial nucleus, it is difficult to find a set of good quantum numbers. The asymptotic or Nilsson quantum numbers, $K^{\pi}[Nn_z\Lambda]$, are no longer conserved and hence are no longer useful for providing a unique label for a state.

### 2.2.4. The Cranked Shell Model (CSM)

At very high spins, when the Coriolis and centrifugal forces strongly perturb the wave-functions of many nucleons, a better description of the single-particle energies is provided by the Cranked Shell Model. CSM is a full microscopic description of the rotating nucleus and was first proposed by Inglis [12, 13] and later by Bengtsson and Frauendrof [14]. The principal assumptions of CSM are that the nuclear mean field in the intrinsic frame is static and unchanged by any rotation, and that the rotation affects only the

energies of the single-particle (and quasiparticle) orbits. The nucleons are thought of as independent particles moving in a deformed potential well which is rotating with the intrinsic coordinate frame at fixed rotational frequency $\omega$. The nucleus is modelled as sitting in a potential that is rotating about a fixed axis, normally to the x-axis. The calculations are carried out in the rotating frame, making it necessary to convert the Hamiltonian to this frame by operating on to with the operator,

$$R_x = \exp\left[-iI_x\omega t\right], \tag{2.35}$$

where, $I_x$ is the projection of the total angular momentum onto the rotation axis, $x$. This gives a Hamiltonian of the form,

$$H' = H_0 - \omega J_x, \tag{2.36}$$

where, $H_0$ is the Hamiltonian of the oscillator potential in the laboratory frame and the $\omega J_x$ term is known as the cranking term. The cranking term includes the effects of the rotational forces acting on any orbiting nucleons that are the Coriolis and centrifugal forces. The Coriolis force acts to align the angular momentum of the nucleons with the rotation ($x$) axis. The Hamiltonian, $H'$, is the Hamiltonian in a frame of reference rotating with an angular frequency $\omega$ about the $x$-axis. The eigenvalues of this Hamiltonian are known as Routhians and the lowest eigenstate of $H'(\omega)$ correspond to an yrast state.

The inclusion of the cranking term $-\omega J_x$, lifts the degeneracy seen in the Nilsson single-particle orbits and breaks the time-reversal symmetry. This means that the only symmetries conserved are parity, $\pi$ and signature.

### 2.2.4.1. Nuclear Spin and Parity

The total angular momentum of a nucleon, $j$ is defined as the coupled sum of the orbital angular momentum, $i$ and spin, $s$: $j = l + s$. The total angular momentum (or nuclear spin), $I$ of a nucleus is the vector sum of the total angular momenta of all the nucleons. The following rules [15] apply: $I$ is a half integer and $I$ is an integer for odd-A and even-A nuclei respectively. The parity quantum number $\pi$ is defined as the eigenvalue of the reflection operator through the origin. If the parity operator $\hat{\pi}$ acts on a wavefunction $\Psi(x)$, such that:

$$\hat{\pi}\Psi(x) = \Psi(-x) = +\Psi(x), \tag{2.37}$$

and

$$\hat{\pi}\Psi(x) = \Psi(-x) = -\Psi(x), \tag{2.38}$$

It implies that the wavefunction have even (unchanged) and odd (changed by inversion) parities respectively. Parity quantum number is expressed as $\pi = \pm 1$, which are the eigenvalues of the parity operator, $\hat{\pi}$. The parity associated to a single-particle level is determined by its orbital angular momentum as $\pi = (-1)^l$. The total parity of the nucleus is determined by the product of the parities of all occupied levels. Therefore, knowing the nuclear spin and parity, nuclear states can then be labelled according to the notation: $I^{\pi}$.

### 2.2.4.2. Signature

Signature is a quantum number which is conserved in the rotational frame. It is associated with the rotational invariance of an axial system with respect to the plane perpendicular to the axis of symmetry. The eigenvalues of the rotation operator given in Eq$^{n}$. 2.35 are given by,

$$r_x = \exp[-i\pi\alpha], \tag{2.39}$$

where, $r_x = r$ is the signature quantum number. The phase factor associated with signature is,

$$r = (-1)^I, \tag{2.40}$$

and, therefore, for a $\Delta I = 1$rotational band, the odd and even numbered spins will have opposite signatures. For multi-quasiparticle configurations, the signature is constrained by the definition,

$$I = \alpha mod 2 \tag{2.41}$$

The exponent of $r$, $\alpha$ is usually preferred over $r$ as it is an additive quantity. The angular momenta and signatures or rotational bands are related as follows.

$$\begin{aligned} I &= 0,2,4 \quad for\ \alpha = 0, r = +1, \\ I &= 1,3,5 \quad for\ \alpha = 1, r = -1, \\ I &= \tfrac{1}{2}, \tfrac{5}{2}, \tfrac{9}{2} \quad for\ \alpha = +\tfrac{1}{2}, r = -i, \\ I &= \tfrac{3}{2}, \tfrac{7}{2}, \tfrac{11}{2} \quad for\ \alpha = -\tfrac{1}{2}, r = +i, \end{aligned} \tag{2.42}$$

The values of signature restrict the allowed spin values in rotational bands. Signature remains a good quantum number even when $K$ is not and hence is useful for describing axially asymmetric systems.

The removal of the degeneracy by the $-\omega J_x$ term in the cranked Hamiltonian means that the two different signatures of a band can have different energies. This effect is known as signature splitting. This splitting is increased with rotational frequency and orbitals with a low-Ω projection experience larger signature splitting. It is also observed in the rotation-aligned limit, as these bands also exhibit a large signature splitting.

### 2.2.5. Potential Energy Surface (PES) Calculations

PES type calculations minimise the potential energy of the nucleus as a function of a given nucleon configuration, rotational frequency and the nuclear deformation parameters. The evolution of nuclear shape may thus be predicted within the framework of PES calculations which employ the CSM. However the CSM carries with it the main deficiency of phenomenological shell model, namely the inability to reproduce nuclear bulk properties. It is thus unable to accurately predict the binding energy, and hence the nuclear potential energy. On the other hand the liquid drop model (LDM) [16, 17] successfully predicts bulk properties that depend smoothly on nuclear number, but cannot account for contributions to the binding energy that arise from shell effects.

### 2.2.6. Total Routhian Surface (TRS) Calculations

Although the cranked shell model tells us what happens to the energies of the single particle orbits under rotation using a fixed set of deformation parameters, it does not provide information about what this set of parameters if likely to be. Potential energy surface calculations are very useful, and are performed to find which deformations are energetically favourable at a given rotational frequency or angular momentum.

TRS calculations are based on the cranked shell model and involve calculating the total Routhain at a pre-determined rotational frequency. The surface is generated by performing the calculations at various points in the deformation plane ($\beta_2$,$\gamma$). As the rotating frame of reference increases in rotational frequency, the parameters defining the system may change. Total Routhian surface calculations [18] aim to find a minimum in the total nuclear energy at a particular rotational frequency. The lattice of points is known as a mesh, and the resultant surface shows peaks and troughs, the troughs corresponding to minima which are stable deformations.

The energy of the nucleus is dependent on the deformation parameters $\beta_2$, $\beta_4$ and γ. The total energy of the nucleus is calculated using the Strutinsky method [19 - 21],

combining the liquid-drop and single-particle energies. The Routhians are then plotted in a contour plot in deformation space, allowing the minima to be clearly seen. Often, more than one potential minimum is present, each one corresponding to a different nuclear shape. The deformation parameters corresponding to the shape changes can be determined from the contour plots. The deformation parameters determined for different rotational frequencies can then be used to carry out cranked shell model calculations to produce quasiparticle plots. From these quasiparticle plots the values of $i$ and $e'$ can be determined for a particular configuration.

The total routhian $E^{\omega}_{tot}(Z,N,\hat{\beta})$ of a nucleus (Z,N) at a frequency ω and a deformed $\hat{\beta}$ is obtained within the Woods-Saxon Bogolyubov – Struinsky approach. It expressed as the sum of the macroscopic liquid drop energy, the shell-correction energy and the pairing energy.

$$E^{\omega}(Z,N,\beta) = E^{\omega_{macr}}(Z,N,\beta) + \delta E^{\omega_{shell}}(Z,N,\beta) + \delta E^{\omega_{pair}}(Z,N,\beta), \quad (2.43)$$

This equation can be re-written as:

$$E^{\omega}(Z,N,\beta) = E^{\omega=0}(Z,N,\beta) + [\langle\psi^{\omega}|H^{\omega}(Z,N,\beta)|\psi^{\omega}\rangle - \langle H^{\omega=0}(Z,N,\beta)\rangle_{BCS}] \quad (2.44)$$

Here $E^{\omega=0}(Z,N,\beta)$, represents the liquid drop energy, the single particle shell correction defines by the Strutinsky averaging procedure, and the Bardeen, Cooper, Schrieffer (BCS) pairing energy at zero frequency. The term in the bracket corresponds to the change in energy due to deformation.

**References**


1. K.E.G. Löbner *et al.,* Nucl. Data. Tables 7, 495 (1970)
2. G. Anderson, *et al.,* Nucl. Phys. A 368, 205 (1976)
3. W. Greiner and J.A. Maruhn, *Nuclear Models*, Springer, (1995)
4. N. Jelly, *Fundamentals of Nuclear Physics*, Cambridge University Press, (1990)
5. R.F. Casten, *Nuclear Structure from a Simple Perspective*, 2nd edition, Oxford Science Publications, (2000)
6. B.T. Feld, Ann. Rev. Nucl. Sci. 2, 239 (1953)
7. C.H. Townes, H.M. Foley, W. Low. Phys. Rev. 76, 1415 (1949)
8. J. Rainwater, Phys. Rev. 79, 432 (1950)
9. S.G. Nilsson, Dan. Mat-Fys. Medd. 29, 16 (1955)
10. R. Firestone, *Table of Isotopes*, 8th edition, Wiley, (1996)
11. S.G. Nilsson and I. Ragnarsson, *Shapes and Shells in Nuclear Structure*, Cambridge University Press, (1995)
12. D.R. Inglis, Phys. Rev. 96, 1059 (1954)
13. D.R. Inglis, Phys. Rev. 103, 1786 (1956)
14. R. Bengtsson, S. Frauendrof, Nucl. Phys., A 327, 139 (1979)
15. K.S. Krane, *Introductory Nuclear Physics*, Wiley, (1988)
16. H.A. Bethe and R.F. Bacher, Rev. Mod. Phys. 8, 82 (1936)
17. C. von Weizsacker, Z. Phys. 96, 431 (1935)
18. W. Nazarewicz, G.A. Leander, J. Dedek, Nucl. Phys., A 467. 437 (1987)
19. V.M. Strutinsky, Nucl. Phys. A 95, 420 (1967)
20. V.M. Strutinsky, Nucl. Phys. A 122, 1 (1968)
21. V.M. Strutinsky, Nucl. Phys. A 188, 225 (1972)